RAPID COMMUNICATION

Journal
The American Ceramic Society

Micro-scale mechanical properties of surface layer in ion-exchanged glass

Saho Fujita[1] | **Tatsuki Ohji**[1,2] | **Tsukaho Yahagi**[3] | **Motoyuki Iijima**[1] | **Junichi Tatami**[1]

[1]Yokohama National University, Yokohama, Japan

[2]National Institute of Advanced Industrial Science and Technology (AIST), Nagoya, Japan

[3]Kanagawa Institute of Industrial Science and Technology, Ebina, Japan

Correspondence
Tatsuki Ohji, National Institute of Advanced Industrial Science and Technology (AIST), Sakurazaka 4-205, Moriyama-ku, Nagoya, Aichi, 463-8560, Japan.
Email: t-ohji@aist.go.jp

Abstract

Today, ion-exchanged or chemically strengthened glass is ubiquitously used all over the world, typically for scratch-free display cover of personal mobile phones. It has been known that the strengthening is due to developments of high compressive stress in the surface layer by its internally constrained dilation . We investigated micro-scale mechanical properties of the surface layer itself of a Na^+-to-K^+ ion-exchanged soda lime silicate glass, revealing that the strength of the layer increased nearly 40% by the ion-exchange with little compression effect from the interior. The fracture toughness, however, was comparable before and after the ion-exchange, indicating that the ion-exchange reduces the crack size of the fracture origin. Theoretical estimates of fracture surface energies verified the measured fracture toughness. It was presumed that the observed crack-size reduction is due to crack healing effects enhanced by the ion-exchange.

KEYWORDS
crack healing, fracture toughness, glass, ion-exchange, mechanical properties, strength, surface energy

1 | INTRODUCTION

Chemical strengthening of glass by ion exchange below glass transition temperature is one of the most effective techniques for improving the mechanical properties of glass products.[1–8] In this process, an alkali-containing glass is immersed in a molten salt bath containing larger alkali ion. The larger invading alkali ions from the salt bath replace the smaller host alkalis nearby to the glass surface, leading to development of high compressive surface layer. This layer can play a role of suppressing crack formation in the glass surface and increasing its strength substantially.[2,3] The advantages of this process include introduction of relatively high surface compression, applicability to thin plates (even 100 μm) and irregular-shaped products, with no measurable optical distortion, and so forth.[2] Currently, chemically strengthened glass is being

used for broad applications, especially scratch-free display cover of billions of personal telecommunication devices among them.[6–8]

Correct evaluation of the mechanical performance of the surface layer of chemically strengthened glass is essential for ensuring its reliable use. Nano-indentation technique has been most frequently employed for this purpose.[9–11] Calahoo et al.[9] investigated mechanical properties as a function of case depth in ion-exchanged glasses using nano-indentation and reported significant enhancements in Young's modulus and hardness near the surface attributable to compressive stress, and so forth. Karlsson[10] and Karlsson et al.[11] studied mechanical, thermal, and structural properties of chemically strengthened soda lime silicate glasses using nano-indentation, revealing, for example, substantial dependence of hardness, elastic modulus, crack resistance on the SiO_2, CaO, and TiO_2

content.[10] The properties measured by nanoindentation methods, however, are always subject to the surface compression. It is critically important to reveal their intrinsic values free from such compressive residual stress.

The microcantilever bending test is a powerful technique that can measure mechanical properties at a micro-scale under tensile stress.[12–21] A load is applied at the tip of a microcantilever beam specimen to generate the bending stress on the top surface of the specimen. This method has been employed for investigating micro-scale mechanical performance of various inorganic materials including silicon nitride,[12–14] silicon carbide,[15] silicon,[16] zirconia,[17,18] alumina,[19] hydroxyapatite,[20] and high-entropy carbide.[21] The specimen thickness is typically two to three microns, while the case depth or the depth of the surface compression of ion-exchanged glass is usually several to several ten microns. Therefore, it is possible to measure the above-mentioned intrinsic mechanical properties of the ion-exchanged layer.

In this study we investigated micro-scale mechanical properties including fracture strength, fracture toughness, and Young's modulus for the ion-exchanged layer of a chemically strengthened soda lime silicate glass using microcantilever bending tests.

2 | EXPERIMENTAL PROCEDURE

2.1 | Sample preparation and ion exchange

This study used a commercially available soda lime silicate float glass (AGC Inc.) as the sample material. Its nominal chemical composition was 71.5 wt% SiO_2–13.2 wt% Na_2O–8.3 wt% CaO–4.4 wt% MgO–1.9 wt% Al_2O_3–0.4 wt% K_2O–0.2 wt% SO_3 in addition to impurities (<0.2 wt%) related to Fe, Ti, and so forth. Thus, we assume the following molar ratio: 70.6 mol% SiO_2–12.6 mol% Na_2O–8.8 mol% CaO–6.4 mol% MgO–1.1 mol% Al_2O_3–0.3 mol% K_2O–0.2 wt% SO_3 (hereafter, $12.6Na_2O·8.8CaO·6.4MgO·1.1Al_2O_3·0.3K_2O·0.2SO_3 ·70.6SiO_2$). The glass was cut into a square plate of $10 \times 10 \times 0.8$ mm, and mirror polishing (mirror-like finish by buffing a specimen surface with diamond slurry) was made, followed by ion-milling process (Ilion Model 693, Gatan, Inc.), to obtain a flat and smooth surface.

The ion exchange was performed by immersing this plate in molten KNO_3 (Kanto Chemical Co., Inc., >99.0%) at 435°C for 2 h. The stress in the chemically strengthened layer and the case depth for the ion-exchanged plate were determined to be 600–650 MPa and 6.5 μm,
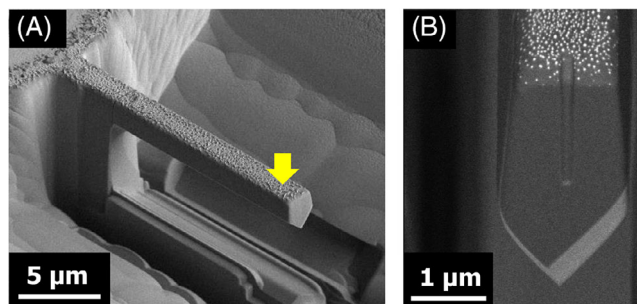

FIGURE 1 Microcantilever beam specimen: (A) general view and (B) front view. The yellow arrow indicates the loading point (A). A small indent was made to determine the loading point (B).

respectively, using a surface stress measuring device by photoelasticity (FSM-6000, Irie Corporation). Although the precise stress-distribution along the depth was not measured by this technique, it can be assumed that the stress monotonously decreases with the depth because of the limited ion-exchange time.[22]

2.2 | Microcantilever bending tests

Microcantilever beam specimens were prepared from both the untreated and ion-exchanged glass plates using an focused ion beam (FIB) technique (XVision 200 TB, SII NanoTechnology Inc.) with an acceleration voltage of 30 kV and beam currents of 27, 6.5, and 1.3 nA. A thin osmium coating was applied to the glass plates using an osmium coater (HPC-1SW, Vacuum Device Inc.) before machining to avoid electric charge-up. For the ion-exchanged samples, the chemically treated surface was made the top surface of the beam specimen, where the maximum tensile stress occurs in the bending tests. Figure 1 shows scanning electron microscope (SEM) images of the microcantilever beam specimen. The debris observed on the top surface of the specimen is the remains of the above-stated osmium coating. While it is known that an osmium coating causes little damage to samples compared with other techniques such as a carbon coating, the influence of this debris on the mechanical behavior is unknown. The degree of the influence, however, will be almost the same between the untreated and ion-exchanged samples, if any. The specimens had a pentagonal section profile, and their width and thickness ranged in 1–2 μm and 2–3 μm, respectively, with an approximate length of 15 μm. The sectional shape and sizes of each specimen were determined precisely for rigorous calculation of the second moment of area by SEM observation. The load was applied at a point 12 μm from the end of the specimen at a loading rate of 100 μN/s using a nano-indenter with a Bercovich-type diamond (temperature of 23°C and relative
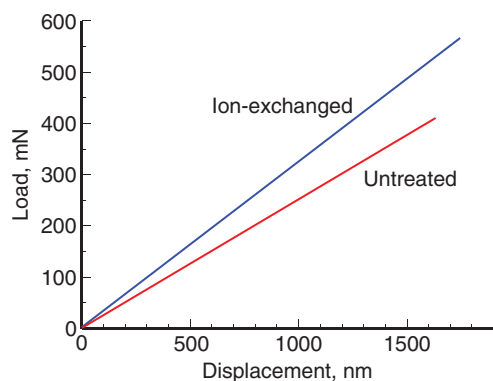
FIGURE 2 Examples of load–displacement diagrams obtained in microcantilever bending tests for untreated and ion-exchanged glass specimens.

TABLE 1 Mechanical properties determined by microcantilever bending tests for the untreated and ion-exchanged glasses.

	Untreated	Ion-exchanged
Bending strength (GPa)	3.04 ± 0.19	4.27 ± 0.35
Young's modulus (GPa)	74.4 ± 3.8	98.3 ± 9.5
Fracture toughness (MPa.m$^{1/2}$)	0.81	0.83

Note: The number of specimens is nine for each bending strength and Young's modulus measurements and is one for each fracture toughness.

humidity of 50%). The bending strength and Young's modulus of the specimen were calculated from the load and displacement of the bending tests. For samples of fracture toughness measurements, a sharp notch with a depth of approximately 200 nm and a tip radius less than 15 nm was introduced by FIB machining at the fixed end of the beam, and they were measured by SEM observation. Loading tests similar to the bending strength measurements were carried out. To estimate the fracture toughness, FEM analysis was performed using the specimen geometry, notch depth, and fracture load. The detailed procedure for determining the bending strength, Young's modulus and fracture toughness is described in the Supporting Information.

3 | RESULTS AND DISCUSSION

3.1 | Measured mechanical properties

All the load–displacement diagrams obtained in the microcantilever bending tests for both the ion-exchanged and untreated glass specimens show linear relationships until the final failure, as shown in Figure 2. The brittle failure characteristics indicate a catastrophic crack propagation from a preexisting defect, which is typical of glass materials, even in such minute specimens.

Table 1 shows the mechanical properties determined by the microcantilever bending tests for the untreated and ion-exchanged glasses. Nine specimens were used for each bending strength and Young's modulus measurements. The bending strength of the untreated glass is 3.04 GPa, which increases to 4.27 GPa after the treatment, indicating an about 40% (>1.2 GPa) improvement. It should be noted, however, that, as stated in the experimental procedure, the case depth of the chemically strengthened layer is 6.5 μm, and that the compressive stress monotonously

decreases with the depth. Because the specimen's thickness is 2–3 μm, the microcantilever beam is still subjected to some residual stress. Assuming a linear reduction of the stress, the difference of the residual stress between the top surface and bottom portion is estimated to be 30%–40% of 650 MPa, which is roughly 200–300 MPa. Because of the stress balance between the top and bottom, a compressive stress of about 100–150 MPa remains at the top surface. Thus, it can be presumed that the real bending strength of the ion-exchanged glass is 100–150 MPa lower than 4.27 GPa.

In term of the fracture toughness, both the untreated and ion-exchanged samples show similar values (Table 1). Because of the difficulty of introducing a sharp notch with a uniform depth, and so forth, the measurement was successful with only one specimen for each of the samples. For this reason, we tried to examine the validity of the results by a theoretical estimate, as described in Section 3.2. Tatami et al.[23] reported, however, that the standard deviation of the fracture toughness values measured by this technique for other kinds of commercially available soda lime glasses (with >6 specimens for each) ranged between 4% and 12%.

The brittle fracture characteristics (Figure 2), the bending strength, σ_f, and the fracture toughness, K_{IC}, can be related to the crack size of the fracture origin. Assuming a surface crack whose depth is C_L in a semi-infinite two-dimensional body, they are related by:

$$\sigma_f = \frac{K_{IC}}{1.12\sqrt{\pi C_L}} \tag{1}$$

The calculated C_L is 18 and 9.6 nm for the untreated and ion-exchanged samples, respectively, implying that the crack size is reduced to 53%. It should be noted that the crack size is so small that it is uncertain whether they meet strictly the criteria of small scale yielding of linear fracture mechanics, allowing only a relative comparison. From this result, it can be presumed that the ion-exchange treatment exerts some effect to reduce the sizes of the preexisting cracks or defects.

TABLE 2 (A) Bond dissociation energies Si–O, Na–O, K–O, Ca–O, Mg–O, Al–O, and S–O. (B) Molar mass and density of SiO_2, Na_2O, K_2O, CaO, MgO, Al_2O_3, and SO_3 (from Lide[26]).

(A)							
	Si–O	**Na–O**	**K–O**	**Ca–O**	**Mg–O**	**Al–O**	**S–O**
Bond energy (kJ/mol)	799.6	270	271.5	383.3	502	501.9	517.9
(B)							
	SiO_2	**Na_2O**	**K_2O**	**CaO**	**MgO**	**Al_2O_3**	**SO_3**
Molar mass (g/mol)	60.09	61.98	94.20	56.08	40.30	101.96	80.06
Density (g/cm³)	2.196	2.27	2.35	3.34	3.6	3.99	1.92

3.2 | Theoretical fracture surface energy and fracture toughness

In contrast to the large increases of the bending strength and Young's modulus, the fracture toughness, K_{IC}, showed a slight improvement. K_{IC} is related to facture surface energy, γ, by the following equation, if the fracture or crack extension occurs in stable manner with plane strain conditions.

$$K_{IC} = \sqrt{\frac{2\gamma E}{(1 - \nu^2)}} \tag{2}$$

where E is the Young's modulus and ν is the Poisson's ratio. Rouxel et al.[24,25] proposed a model to predict γ and K_{IC} of ionocovalent glasses from their nominal compositions and showed a remarkable agreement between the theoretical and experimental values. Here, using this model, we try to deduce γ and K_{IC} from the compositions and compare them with the measured ones. In the model, γ is obtained from the surface density of representative structural units and the relevant bond strength, by considering the number and the type of bonds involved in the fracture process as the crack proceeds through the considered structural unit, as follows[24,25]:

$$\gamma = \frac{1}{2}\left(\frac{\rho}{M_0}\right)^{2/3} \mathcal{N}^{-1/3} \sum_i x_i n_i U_{oi} \tag{3}$$

where ρ and M_0 are the glass density (specific gravity) and the molar mass of a representative unit (gram-atom of glass), $\mathcal{N}$ is Avogadro number, x_i is the stoichiometric fraction of the species involved in the ith bonding energy U_{oi} between the ith cation and its nearest neighbor oxygen anion in case of an oxide glass, and n_i is the number of such bonds supposed to be broken as the crack front propagates to the next unit.

For U_{oi}, we used the bond dissociation energies as listed in Table 2A.[26] Table 2B also shows the molar mass and density of each compound used for the calculation,[26] while x_i was determined from the molar

TABLE 3 Fracture surface energy, γ, and fracture toughness, K_{IC}, theoretically estimated for the untreated ($12.6Na_2O \cdot 8.8CaO \cdot 6.4MgO \cdot 1.1Al_2O_3 \cdot 0.3K_2O \cdot 0.2SO_3 \cdot 70.6SiO_2$ [mol%]) and ion-exchanged ($12.9K_2O \cdot 8.8CaO \cdot 6.4MgO \cdot 1.1Al_2O_3 \cdot 0.2SO_3 \cdot 70.6SiO_2$ [mol%]) glasses in as melted (fully relaxed) and semi-relaxed states.

	Untreated	Ion-exchanged
Surface energy (J/m²), (as melted)	3.40	3.27
Fracture toughness (MPa.m^{1/2}), (as melted)	0.735	0.828
Surface energy (J/m²), (semi-relaxed)	–	3.34
Fracture toughness (MPa.m^{1/2}), (semi-relaxed)	–	0.836

ratio of the composition. The obtained γ values for the $12.6Na_2O \cdot 8.8CaO \cdot 6.4MgO \cdot 1.1Al_2O_3 \cdot 0.3K_2O \cdot 0.2SO_3 \cdot 70.6SiO_2$ (in mol%) and for the $12.9K_2O \cdot 8.8CaO \cdot 6.4MgO \cdot 1.1Al_2O_3 \cdot 0.2SO_3 \cdot 70.6SiO_2$ (replacing Na_2O with K_2O) are shown in Table 3. Here, it was assumed that Na^+ ions are completely exchanged for K^+ ions, though the Na–K ion-exchange process is known to be often hindered by a very small amount of impurity, such as Ca and Mg, in the potassium nitrate salt bath.[27] Substituting the measured Young's modulus into Equation (2), we obtain K_{IC} values also listed in Table 3. The Poisson's ratio was assumed to be 0.25 from its relationship with the atomic packing density,[28] which was calculated using the study by Rouxel.[24] It should be noted that these values are based on the assumption that the glass is as melted.

In reality, however, due to the network dilation anomaly, the invading K^+ ions do not obtain the fully relaxed environments but are constrained from expansion to some extent by the preexisting glass structure (hereafter, this state is denoted as "semi-relaxed"). Tandia et al.[29] estimated the molar volume changes when replacing Na_2O with K_2O for an as-melted glass of $xNa_2O \cdot (20-x)K_2O \cdot 20Al_2O_3 \cdot 60SiO_2$ (mol%). When

$x = 12$–13 mol%, which corresponds to the ion exchange of this study, the ratio of the network dilation coefficient of the as-melted glass is 50%.[29] Considering this effect for the calculation of M_0 in Equation (3), we obtain γ and K_{IC} in semi-relaxed state, as listed in Table 3.

Comparing the K_{IC} values theoretically predicted (Table 3) and experimentally measured (Table 1), there is a very good agreement for the ion-exchanged sample, while the former is slightly higher than the latter for the untreated one (though the difference is still <0.1 MPa m$^{1/2}$). Here, we recalculate C_L in Equation (1), using the theoretical K_{IC} values of Table 3 (semi-relaxed one for ion-exchanged). The result is $C_L = 15$ and 9.7 nm for the untreated and ion-exchanged samples, respectively, indicating that the size of the preexisting crack of the fracture origin is reduced to 65%. In the previous Section 3.1, the real bending strength of the ion-exchanged glass is presumed to be 4.1–4.2 GPa. Taking this into consideration, C_L increases to 10 nm for the latter, resulting in some 67% reduction.

Macrelli[30] evaluated strength of soda lime silicate float glasses before and after ion-exchange using a linear fracture mechanics model and compared the result with experimental data obtained in macroscopic tests, revealing that the latter was higher than the former. For explaining the difference, he introduced a surface-flaw severity reduction factor, which was estimated at 69% when assuming a stress relaxation. This value is relatively close to the above flaw size reduction, 65%–67%.

3.3 | Crack-size reduction and crack healing

One of the most plausible reasons for the crack size reduction is crack healing. When ceramic materials including glass are heat-treated under appropriate conditions (temperature, humidity, pressure, residual stress, etc.), complex physical and chemical reactions will promote various phenomena such as diffusion, softening, viscous flow, and volume expansion, resulting in crack self-healing.[31–35] Wilson and Case[32] in-situ observed healing behavior of Vickers indentation cracks in soda-lime-silicate glass at 430°C under different humidity levels, using an environmental SEM. The crack healing was activated with increasing the humidity, and the crack length was reduced to 63% of the initial one at a relative humidity of 64%, after 90 min exposure.

Recently a lot of attention has been paid to humidity or water vapor in glass community, since they exsert huge, positive effects on strengthening glasses.[36–41] Wiederhorn et al.[39–41] revealed that, when water penetrates into silica glass, a pronounced volume expansion occurs by reaction of siloxane bonds of the glass with water to form SiOH. If the dilation occurs in a constrained manner such as at the glass surface, it generates compressive residual stresses at the surface, strengthening the glass significantly. This mechanism is the same as the chemical-strengthening of glass by ion-exchange. Such compressive stresses should enhance activities of crack healing, if the temperature is high enough. The humidity-enhanced crack healing behavior at 430°C[32] is most presumably involved with the volume expansion of glass.

Likewise, in this study, when Na$^+$ ions are replaced with K$^+$ ions at the surface during the ion exchange, surface cracks should receive compressive stresses, which are favorable to crack healing. Particularly, K$^+$ ions in contact with the surface first penetrate into the cracks and invade inside from the crack planes, generating a zone of dilation around and behind the crack tip. This dilated part is constrained from expansion by the surrounding glass, a compressive stress is generated in this dilation zone. Thus, the cracks are most susceptible to the compression, which accelerates crack healing in a manner similar to the above-stated humidity-enhanced crack healing behavior. It is interesting to note that the crack reduction by the humidity-enhanced crack healing (430°C, 90 min, 64% humidity) was 63%, which is very close to those by the ion-exchange in this study, 53% in Section 3.1 and 65%–67% in Section 3.2 (435°C, 120 min), though the dilation mechanisms are different. In conclusion, we think that the crack-size reduction observed in this study is most likely due to the crack healing effects occurring during the ion-exchange.

4 | SUMMARY

We investigated the micro-scale mechanical properties, including bending strength, fracture toughness, and Young's modulus, for the surface layer of a soda lime silicate glass before and after K$^+$ ions replaced Na$^+$ ions. It was revealed that the strength of the layer increased nearly 40% by the ion-exchange with little compression effect from the interior. The fracture toughness, however, was comparable, indicating that the ion-exchange reduces the crack size of the fracture origin. The degree of the crack-size reduction due to ion-exchange obtained in this study was very close to that predicted by Macrelli[30] from the macroscopic tests. Because of the similarity of the phenomena, it was presumed that the crack-size reduction observed in this study is due to crack healing effects enhanced by the ion-exchange.

ORCID

Tatsuki Ohji https://orcid.org/0000-0002-4880-9138
Junichi Tatami https://orcid.org/0000-0002-4713-460X

REFERENCES

1. Kistler SS. Stresses in glass produced by nonuniform exchange of monovalent ions. J Am Ceram Soc. 1962;45:59–68. https://doi.org/10.1111/j.1151-2916.1962.tb11081.x
2. Varshneya AK. Chemical strengthening of glass: lessons learned and yet to be learned. Int J Appl Glass Sci. 2010;1:131–42. https://doi.org/10.1111/j.2041-1294.2010.00010.x
3. Varshneya AK. The physics of chemical strengthening of glass: room for a new view. J Non-Cryst Solids. 2010;356:2289–94. https://doi.org/10.1016/j.jnoncrysol.2010.05.010
4. Gy R. Ion exchange for glass strengthening. Mater Sci Eng B. 2008;149:159–65. https://doi.org/10.1016/j.mseb.2007.11.029
5. Wondraczek L, Mauro JC, Eckert J, Kühn U, Horbach J, Deubener J, et al. Towards ultrastrong glasses. Adv Mater. 2011;23:4578–86. https://doi.org/10.1002/adma.201102795
6. Mauro JC, Smedskjaer MM. Unified physics of stretched exponential relaxation and Weibull fracture statistics. Physica A. 2012;391:6121–27. https://doi.org/10.1016/j.physa.2012.07.013
7. Welch RC, Smith JR, Potuzak M, Guo X, Bowden BF, Kiczenski TJ, et al. Dynamics of glass relaxation at room temperature. Phys Rev Lett. 2013;110:265901. https://doi.org/10.1103/PhysRevLett.110.265901
8. Mauro JC, Ellison AJ, Pye LD. Glass: the nanotechnology connection. Int J Appl Glass Sci. 2013;4:64–75. https://doi.org/10.1111/ijag.12030
9. Calahoo C, Zhang X, Zwanziger JW. Nanoindentation study of the surface of ion-exchanged lithium silicate glass. J Phys Chem C. 2016;120:5585–98. https://doi.org/10.1021/acs.jpcc.6b00733
10. Karlsson S. Compositional effects on indentation mechanical properties of chemically strengthened TiO_2-doped soda lime silicate glasses. Materials. 2022;15:577. https://doi.org/10.3390/ma15020577
11. Karlsson S, Mathew R, Ali S, Paemurru M, Anton J, Stevensson B, et al. Mechanical, thermal, and structural investigations on chemically strengthened Na_2O–CaO–Al_2O_3–SiO_2 glasses. Front Mater. 2022;9:953759. https://doi.org/10.3389/fmats.2022.953759
12. Tatami J, Katayama M, Ohnishi M, Yahagi T, Takahashi T, Horiuchi T, et al. Local fracture toughness of Si_3N_4 ceramics measured using single-edge notched microcantilever beam specimens. J Am Ceram Soc. 2015;98:965–71. https://doi.org/10.1111/jace.13391
13. Tanabe M, Tatami J, Iijima M, Yahagi T, Takahashi T, Nakano H, et al. Deformation behaviors and fracture strength of β-Si_3N_4 single crystals. J Am Ceram Soc. 2023;106:5431–39. https://doi.org/10.1111/jace.19167
14. Fujita S, Tatami J, Yahagi T, Takahashi T, Iijima M. Degradation evaluation of Si_3N_4 ceramic surface layer in contact with molten Al using microcantilever beam specimens. J Eur Ceram Soc. 2017;37:4351–56. https://doi.org/10.1016/j.jeurceramsoc.2017.01.016
15. Tatami J, Imoto Y, Yahagi T, Takahashi T, Iijima M. Relationship between bending strength of bulk porous silicon carbide ceramics and grain boundary strength measured using microcantilever beam specimens. J Eur Ceram Soc. 2020;40:2634–41. https://doi.org/10.1016/j.jeurceramsoc.2019.12.029
16. Yamaguchi H, Tatami J, Yahagi T, Nakano H, Iijima M, Takahashi T, et al. Dislocation-controlled microscopic mechanical phenomena in single crystal silicon under bending stress at room temperature. J Mater Sci. 2020;55:7359–72. https://doi.org/10.1007/s10853-020-04528-3
17. Norton AD, Falco S, Young N, Severs J, Todd RI. Microcantilever investigation of fracture toughness and subcritical crack growth on the scale of the microstructure in Al_2O_3. J Eur Ceram Soc. 2015;35:4521–33. https://doi.org/10.1016/j.jeurceramsoc.2015.08.023
18. Henry R, Blay T, Douillard T, Descamps-Mandine A, Zacharie-Aubrun I, Gatt JM, et al. Local fracture toughness measurements in polycrystalline cubic zirconia using micro-cantilever bending tests. Mech Mater. 2019;136:103086. https://doi.org/10.1016/j.mechmat.2019.103086
19. Muramoto M, Tatami J, Iijima M, Matsui K, Yahagi T, Takahashi T, et al. Deformation behavior and bending strength of single crystal 8 mol% yttria stabilized zirconia at microscopic scale. J Eur Ceram Soc. 2024;44:1061–69. https://doi.org/10.1016/j.jeurceramsoc.2023.09.042
20. Otsuka Y, Tatami J, Yamamoto I, Iijima M, Ohji T. Micro- and macro-scale strength properties of c-axis aligned hydroxyapatite ceramics. Ceram Int. 2023;49:40158–65. https://doi.org/10.1016/j.ceramint.2023.09.349
21. Csanádi T, Vojtko M, Dankházi Z, Reece MJ, Dusza J. Small scale fracture and strength of high-entropy carbide grains during microcantilever bending experiments. J Eur Ceram Soc. 2020;40:4774–82. https://doi.org/10.1016/j.jeurceramsoc.2020.04.023
22. Macrelli G, Varshneya AK, Mauro JC. Simulation of glass network evolution during chemical strengthening: resolution of the subsurface compression maximum anomaly. J Non-Cryst Solids. 2019;522:119457. https://doi.org/10.1016/j.jnoncrysol.2019.05.033
23. Tatami J, Katayama M, Iijima M, Yahagi T, Takahashi T. Local fracture toughness of soda—lime glass measured using microcantilever beam specimens. New Glass. 2015;30:30–33. https://www.newglass.jp/mag/TITL/maghtml/114-pdf/+114-p030.pdf
24. Rouxel T. Fracture surface energy and toughness of inorganic glasses. Scr Mater. 2017;137:109–13. https://doi.org/10.1016/j.scriptamat.2017.05.005
25. Rouxel T, Yoshida S. The fracture toughness of inorganic glasses. J Am Ceram Soc. 2017;100:4374–96. https://doi.org/10.1111/jace.15108
26. Lide DR. CRC handbook of chemistry and physics. 89th ed. New York: CRC Press; 2009
27. Sglavo VM. Chemical strengthening of soda lime silicate float glass: effect of small differences in the KNO_3 bath. Int J Appl Glass Sci. 2015;6:72–82. https://doi.org/10.1111/ijag.12101
28. Rouxel T. Elastic properties and short-to medium-range order in glasses. J Am Ceram Soc. 2007;90:3019–39. https://doi.org/10.1111/j.1551-2916.2007.01945.x

29. Tandia A, Vargheese KD, Mauro JC, Varshneya AK. Atomistic understanding of the network dilation anomaly in ion-exchanged glass. J Non-Cryst Solids. 2012;358:316–20. https://doi.org/10.1016/j.jnoncrysol.2011.09.034

30. Macrelli G. Chemically strengthened glass by ion exchange: strength evaluation. Int J Appl Glass Sci. 2018;9:156–66. https://doi.org/10.1111/ijag.12291

31. Wiederhorn SM, Townsend PR. Crack healing in glass. J Am Ceram Soc. 1970;53:486–89. https://doi.org/10.1111/j.1151-2916.1970.tb15996.x

32. Wilson BA, Case ED. Effect of humidity on crack healing in glass from in-situ investigations using an ESEM. J Mater Sci. 1999;34:247–50. https://doi.org/10.1023/A:1004484901369

33. Girard R, Faivre A, Despetis F. Influence of water on crack self-healing in soda-lime silicate glass. J Am Ceram Soc. 2011;94:2402–7. https://doi.org/10.1111/j.1551-2916.2011.04517.x

34. Wang C, Wang H, Shen L, Hou J, Xu Q, Wang J, et al. Numerical simulation and experimental study on crack self-healing in BK7 glass. Ceram Inter. 2018;44:1850–58. https://doi.org/10.1016/j.ceramint.2017.10.121

35. Osada T, Kamoda K, Mitome M, Hara T, Abe T, Tamagawa Y, et al. A novel design approach for self-crack-healing structural ceramics with 3D networks of healing activator. Sci Rep. 2017;7:17853. https://doi.org/10.1038/s41598-017-17942-6

36. Lezzi PJ, Xiao QR, Tomozawa M, Blanchet TA, Kurkjian CR. Strength increase of silica glass fibers by surface stress relaxation: a new mechanical strengthening method. J Non-Cryst Solids. 2013;379:95–106. https://doi.org/10.1016/j.jnoncrysol.2013.07.033

37. Lezzi PJ, Seaman JH, Tomozawa M. Strengthening of E-glass fibers by surface stress relaxation. J Non-Cryst Solids. 2014;402:116–27. https://doi.org/10.1016/j.jnoncrysol.2014.05.029

38. Lezzi PJ, Tomozawa M. An overview of the strengthening of glass fibers by surface stress relaxation. Int J Appl Glass Sci. 2015;6:34–44. https://doi.org/10.1111/ijag.12108

39. Wiederhorn SM, Fett T, Rizzi G, Fünfschilling S, Hoffmann MJ, Guin JP. Effect of water penetration on the strength and toughness of silica glass. J Am Ceram Soc. 2011;94:s196–s203. https://doi.org/10.1111/j.1551-2916.2011.04530.x

40. Wiederhorn SM, Yi F, LaVan D, Richter LJ, Fett T, Hoffmann MJ. Volume expansion caused by water penetration into silica glass. J Am Ceram Soc. 2015;98:78–87. https://doi.org/10.1111/jace.13264

41. Wiederhorn SM, Rizzi G, Wagner S, Hoffmann MJ, Fett T. Stress-enhanced swelling of silica: effect on strength. J Am Ceram Soc. 2016;99:2956–63. https://doi.org/10.1111/jace.14300

SUPPORTING INFORMATION

Additional supporting information can be found online in the Supporting Information section at the end of this article.